Hindawi
Scientific Programming
Volume 2022, Article ID 5726718, 9 pages
https://doi.org/10.1155/2022/5726718

Research Article

Analysis on Transmission Characteristics of Stimulated Raman Scattering Based on the Multi-Sensor Signal Enhancement Technique

Wentao He and Zhiwei Men

College of Physics Jilin University, Changchun, Jilin 130012, China

Correspondence should be addressed to Wentao He; hewt19@mails.jlu.edu.cn

Received 28 March 2022; Revised 20 April 2022; Accepted 22 April 2022; Published 11 May 2022

Academic Editor: Baiyuan Ding

In recent 20 years, fibre laser system has been developed rapidly and widely used for its high quality, high efficiency, high robustness, and compactness. However, there are still many factors (such as non-linear effect, thermal effect, and mode instability) that limit the further increase of power of fibre laser system. Stimulated Raman scattering (SRS) is one of the main limitations in the transmission process of fibre lasers. It not only reduces the output efficiency of fibre lasers, but also increases the damage risk of reverse Stokes light to the system. Recent studies have shown that SRS in low-mode fibres can lead to quasi-static mode degradation in addition to mode instability. With the introduction of multi-sensor enhancement technology in the fibre field, it becomes an effective means to popularise high-power and high-beam quality fibre lasers. Based on the multi-sensor signal enhancement technology, this paper explores the influence of this technology on the output efficiency of SRS in the mode-reducing fibre laser, which provides a new idea and method for the output efficiency and transmission analysis method of fibre laser.

1. Introduction

In 1961, Snitzer of America Optical developed the world's first fibre laser [1, 2]. With the unique advantages of high conversion efficiency, good beam quality, and compactness, fibre lasers have shown promise for a wide range of applications in earth sciences, strong field physics, atomic and molecular physics, frequency conversion, beam synthesis, and industrial processing. Led by pioneers such as Dr. Charles Kao, Dr. E. Snitzer, Dr. Oleg G. Okhotnikov, and Dr. Valentin Gapontsev, fibre laser technology is constantly evolving and single-mode laser power has reached the 10 kW threshold [3]. However, the special waveguide structure of optical fibres allows the laser energy to be confined mainly within the μm level of the fibre core, and as the laser power of the fibre increases, very high energy densities will develop within the core, causing various harmful non-linear effects [4, 5]. Lawrence Livermore Laboratory (USA) and the National University of Defense Technology (China) have conducted theoretical analyses of the output power limit of laser systems under semiconductor laser (LD) pumping structure and the same band pumping structure, respectively, and the results show that the SRS effect is one of the main factors limiting the power increase, and the same conclusion has been obtained experimentally. In order to achieve high-power laser output, few-mode fibres are widely used in high-power fibre laser systems [6]. Recent results have shown that in few-mode fibres, SRS induces a quasi-static mode degradation in conjunction with the excitation of mode instabilities (TMI), and that the corresponding threshold power is well below the threshold defined in the previous model for limiting the near-diffraction output power [7]. Therefore, effective strategies must be adopted to suppress SRS and improve the output of existing high-power, high-beam quality laser systems.

With the joint efforts of researchers, the understanding of SRS has been deepened, and related inhibition techniques have been developed and summarised. Early reviews on

technologies to improve SRS transmission performance mainly focused on fibre structure and design of long-period Raman suppression gratings [8, 9]. In addition to fibre design, the results also show that the system parameters have a great influence on SRS. Therefore, it is necessary to summarise the influence of each parameter on SRS strength at a general level and study its optimisation direction. At the same time, with the development of technology, new fibre structure design and Raman suppression grating technology emerge and show excellent performance, one of which is multi-sensor enhancement technology [10]. In this paper, the influence of multi-sensor enhancement technology on transmission efficiency characteristics of SRS is analysed, and a fibre structure design and transmission analysis method based on multi-sensor signal enhancement technology are proposed. On this basis, the mechanism of multi-sensor enhancement technology on improving transmission efficiency of fibre laser is further clarified.

2. New Physical Characterisation of the SRS Effect Based on the Multi-Sensor Signal

The semi-classical physical formulation of SRS is that an incident photon of frequency ω_p interacts with a medium of intrinsic frequency ω_v to form a Stokes photon of frequency ω_s and an anti-Stokes photon of frequency ω_a [11–13]. On the one hand, this shifts the energy from the signal light to the Raman scattered light, causing a decrease in the power and energy conversion efficiency of the output beam; on the other hand, as the Stokes light generated by the SRS is bi-directional Stokes light, when the backward Stokes light power reaches a certain value, it increases the risk of damage to the optical components in the laser system, limiting the further increase in the power of the laser system [14, 15]. As a light intensity-dependent non-linear effect, increasing the mode field area with a few-mode fibre can effectively suppress SRS; however, the increased mode field area allows the fibre to support multiple modes. Recent studies have shown that the SRS effect in few-mode fibres leads to mode degradation of the output beam, which can be divided into dynamic mode degradation (i.e., transverse mode instability) and quasi-static mode degradation.

As one of the main limiting factors for the power enhancement of current fibre laser systems, TMI is physically characterised by a sharp degradation of the output laser beam quality after the average power of the output laser reaches a threshold value, with dynamic energy transfer between fundamental modes (FMs) and higher-order modes (HOMs) on the order of kHz, which is manifested by transverse mode instability of the output beam [16]. In Raman fibre amplifiers (RFAs), the quantum loss heat generation during the SRS process can also form thermally refractive index gratings, resulting in TMI in Raman light and leading to dynamic energy coupling between the fundamental and higher-order modes [17, 18]. This phenomenon has also been recently observed in ytterbium-ion-Raman hybrid gain fibre laser systems. However, the experimental results also show that when SRS induces TMI, the distribution of the signal light (Raman-pumped light) shows a lateral temporal instability, while the Raman Stokes light only varies in intensity and the lateral distribution remains unchanged, corresponding to the temporal evolution of the spot shape and the mode decomposition of the signal light as shown in Figure 1. This means that the SRS-induced TMI occurs on signal light rather than Raman light.

Since the formation of TMI requires a certain intensity of thermal loading, SRS-induced TMIs usually occur with a Raman power share greater than 50% [19]. Recently, another type of quasi-static mode degradation has been observed in cases where the Raman power share is relatively low (see Figure 2). Experimentally, when the Raman power share reaches 3%, the output laser beam quality degrades rapidly and the spot appears jittered. This phenomenon can be effectively suppressed by suppressing the SRS [20]. The time-domain signal results show corresponding eigenfrequencies in the order of Hz. There are currently two explanations for the physical mechanism of quasi-static mode degradation caused by SRS: one is the coupling of energy from the fundamental mode of the signal light to the higher-order mode of the Raman light due to the inter-mode mixing (IM-WM) effect; the other is the mode degradation of the signal light due to the core-pumped Raman effect.

3. Analysis Method on Transmission Characteristics of SRS Based on the Multi-Sensor Signal Enhancement Technique

On the one hand, the new physical characterisation of SRS in few-mode fibres further limits the power enhancement of high-power, high-beam quality fibre laser systems; on the other hand, as a new phenomenon, there is still a lack of a clear and uniform understanding of the mechanisms underlying the transmission properties of SRS in fibres based on multi-sensor enhancement techniques, and experimental results do not fully match the theoretical explanation [21]. The active suppression strategy in SRS can dynamically regulate the Raman intensity, which can help to further investigate the physical mechanism behind this phenomenon. The use of sensors to dynamically modulate the Raman intensity in SRS transmission properties can help to further investigate the physical mechanisms behind this phenomenon. Thus, in view of the fibre optic transmission efficiency bottleneck, it is necessary to systematically review the beneficial effects of multi-sensor signal enhancement techniques on SRS transmission characteristics and further develop relevant transmission analysis ideas and new methods. Based on the structural design of the multi-sensor signal enhancement technology, this paper presents an overview of optical fibre transmission characterisation methods from the perspective of fibre design and system optimisation.

3.1. Optical Sensors. The coupling equation describing the SRS effect in continuous wave operation, neglecting the Raman optical gain of rare earth ions, dispersion, and non-

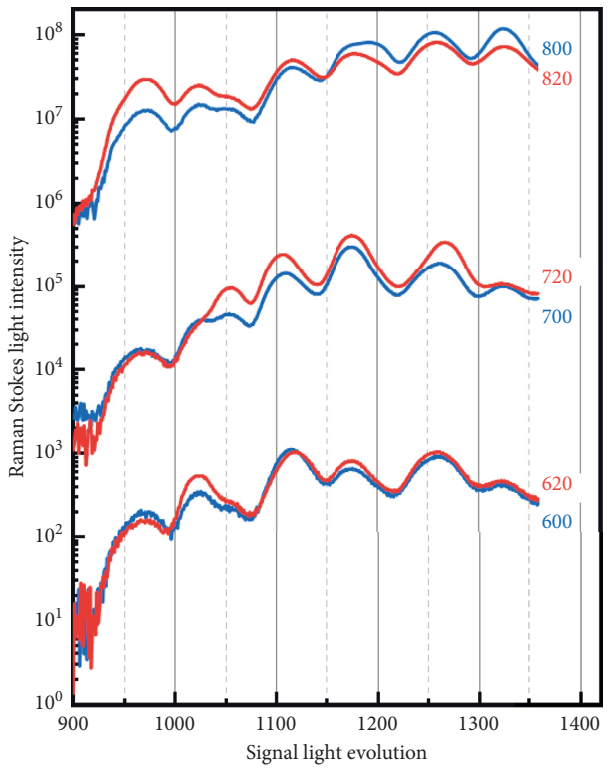

Figure 1: Raman Stokes light intensity corresponding to the temporal evolution of the signal light.

linear effects such as self-phase modulation (SPM) and cross-phase modulation (XPM) on the SRS, can be formulated as

$$\begin{aligned}\frac{dI_R}{dz} &= i_g - i_\alpha,\\ i_g &= g_R I_s I_R,\\ i_\alpha &= \alpha_R I_R,\\ \frac{dI_R}{dz} &= g_R I_s I_R - \alpha_R I_R,\\ \frac{dI_s}{dz} &= -\frac{\omega_s}{\omega_R} g_R I_s I_R - \alpha_s I_s,\end{aligned} \tag{1}$$

where I_s and I_R, are the signal and Raman light intensities; g_R is the Raman gain coefficient; ω_s and ω_R are the signal and Raman light frequencies; and α_s and α_R correspond to the loss factors of the signal and Raman light.

The loss term of Raman light can be expressed as αRIRLeff and the gain term as g RIsIRLeff. Therefore, in order to improve the efficiency of SRS transmission, it is necessary to "increase the Raman loss and decrease the Raman gain, while ensuring the optical power and beam quality of the output signal as much as possible." Compared to increasing the Raman loss, reducing the Raman gain fundamentally reduces the production of Raman light. On the one hand, this improves the transmission efficiency and stability of the system; on the other hand, reducing the gain

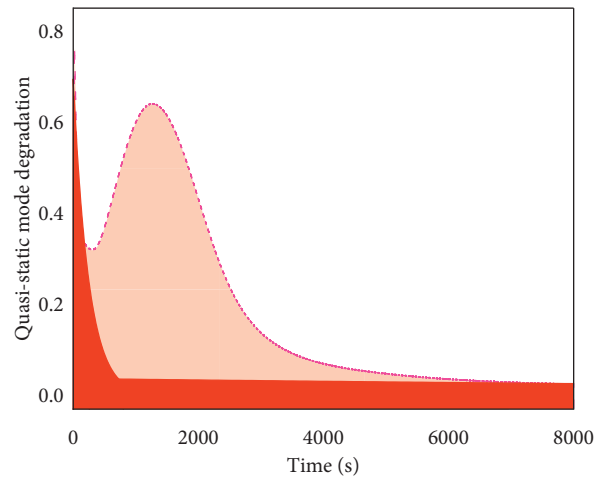

Figure 2: Quasi-static mode degradation with the Raman power share.

also reduces the heat generation due to quantum losses caused by SRS. This is why "Raman light gain reduction" is a common strategy in current optical sensor signalling technology. The latter can be achieved by optical sensors in addition to increasing the core area using large mode field fibres. In addition, the total gain can be reduced by decreasing the effective length of action.

3.1.1. Material Components. Hu et al. [22] suggested that the SRS effect could be suppressed by using Yb: YAG-derived fibres instead of conventional SiO_2 quartz fibres to reduce the Stokes optical gain coefficient. It was shown that an increase in the $Y_2O_3 + Al_2O_3$ content in the fibre leads to a decrease in the Raman gain coefficient, as shown in Figure 3.

In 2021, Sciortino et al. [23] summarised and collated the effect of fibre material on the non-linear effect, stating that the SRS power can be expressed as

$$P_s^R \propto V_m \Lambda^2, \tag{2}$$

where V_m is the molar volume and Λ is the bond compression factor when fibre material is under non-linear effect.

In order to achieve low Raman gain, the fibre material needs to be able to meet the following conditions:

(1) The material is highly disordered, thereby broadening the Raman gain spectrum and reducing the peak.

(2) A material with a high concentration and low gain coefficient g_R is used.

(3) The Raman spectrum of the laser system has minimal overlap with the Raman gain spectrum corresponding to the material components.

3.1.2. Large Mode Field Sensors. As a light intensity-dependent non-linear effect, increasing the mode field area is one of the most effective means of improving the SRS transmission efficiency, which on the one hand leads to a

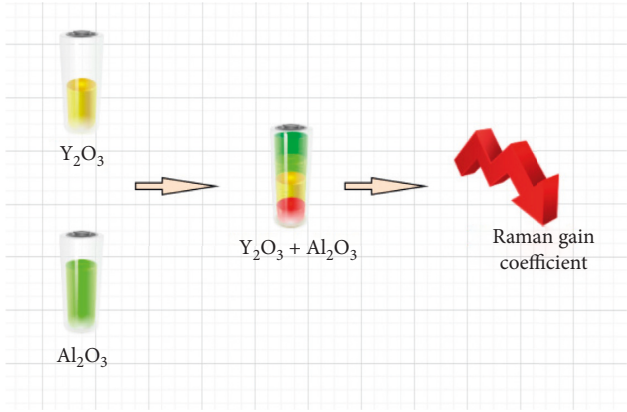

Figure 3: The diagram of the $Y_2O_3 + Al_2O_3$ content in the fibre with the Raman gain coefficient.

reduction in the Raman-pumped light intensity and on the other hand implies a reduction in the effective action distance by increasing the mode field area. In general, the fibre material has a high refractive index, which leads to a further increase in the mode field area of the few-mode fibre, thus causing a decrease in the TMI threshold reduction, which is related to the material used in the fibre. The core of the design of large mode field fibres is therefore to suppress TMI by embedding a large mode field sensor, thus improving the efficiency of the fibre transmission. The most commonly used large mode field sensor fibres are partially doped fibres, tapered fibres, and spindle fibres (SSC). Partially doped fibres are partially doped in the centre to enhance the gain capability of the fundamental mode and achieve higher-order mode suppression through large mode field sensors; tapered fibres have a non-uniform core size distribution along the fibre axis, which can effectively strip higher-order modes and increase the TMI threshold; spindle fibres can be equated to a pair of tapered fibres fused to a section of large mode field fibre. The reduced mode field area at the end of the fibre further improves the output laser beam quality compared to tapered fibres. However, as the output power is further increased to 8.5 kW, the SNR rapidly decreases to 13 dB, limiting the power increase of the laser system.

3.1.3. Off-Domain Sensors. In 2021, Yang et al. [24] designed an Yb-doped ring-distributed filter fibre with the refractive index distribution shown in Figure 4, where the Yb-doped core is enveloped by a high refractive index germanium-doped ring and the preform is ground into a "star" shape. The Yb-doped core is enveloped by a high refractive index germanium-doped ring, and the preform is ground into a "star shape" and coated with a low refractive index polymer to achieve cladding pumping. Figure 5 shows the mode distribution in the fibre, where the unique transverse distribution of the refractive index allows for a different mode distribution of signal light and "noise" such as Raman scattered light, which can be effectively attenuated by reducing the overlap factor between Raman light and signal light. In 2021, Pei et al. [25] introduced a bend-

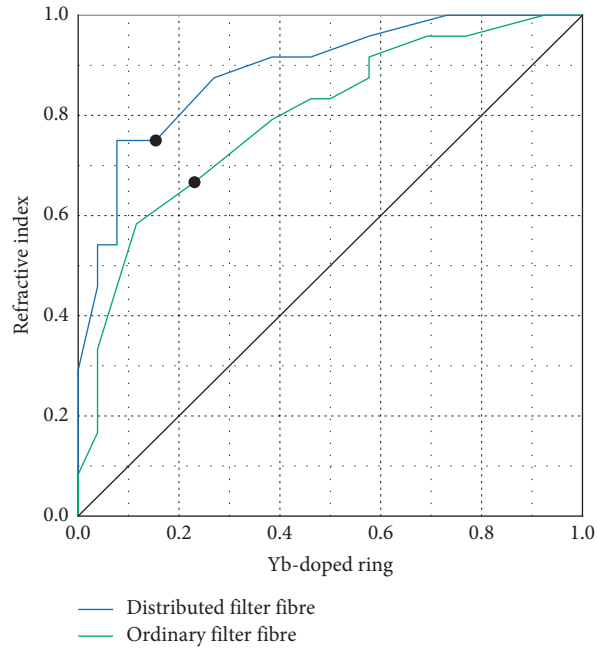

Figure 4: Yb-doped ring-distributed filter fibre with the refractive index distribution.

compensating cladding that allows the fibre to maintain a low gain over a long length, making it possible to use it for long-distance (>20 m) kW-class laser transmission.

3.1.4. Geometric Sensors. The reduction in the perceived length of the geometric sensor is based on the fact that reducing the active length by increasing the absorption coefficient of the gain fibre is an effective strategy for transmission efficiency such as SRS, which can usually be achieved by both increasing the doping concentration of rare earth ions and increasing the area ratio of the inner cladding of the core. However, increasing the doping concentration leads to an enhanced photon darkening effect in the gain fibre which affects the performance of the laser. Increasing the area ratio of the core cladding increases the core area on the one hand, i.e., large mode field fibre technology, and reduces the diameter of the cladding on the other. In 2018, Choi et al. [26] improved the cladding pump absorption by a factor of 1.5 by implanting a fluorine-doped low refractive index quartz rod (LCA) in the inner cladding of a circular double cladding fibre (the fibre structure is shown in Figure 6). In the optical fibre oscillator (OSC), the higher pump absorbance results in a 33% reduction in the effective action distance length compared to a conventional 20/400 μm double-clad fibre (DCF), while the SRS threshold is increased from 1.6 kW to 2.4 kW.

Compared to other transmission efficiency strategies, increasing the mode field area reduces the optical intensity on the one hand and shortens the fibre length on the other, thus providing excellent Raman suppression. High-beam quality laser outputs of 8 kW have been achieved with centrally doped fibres, while high-beam quality laser outputs of 5 kW have also been achieved with spindle fibres. The fact

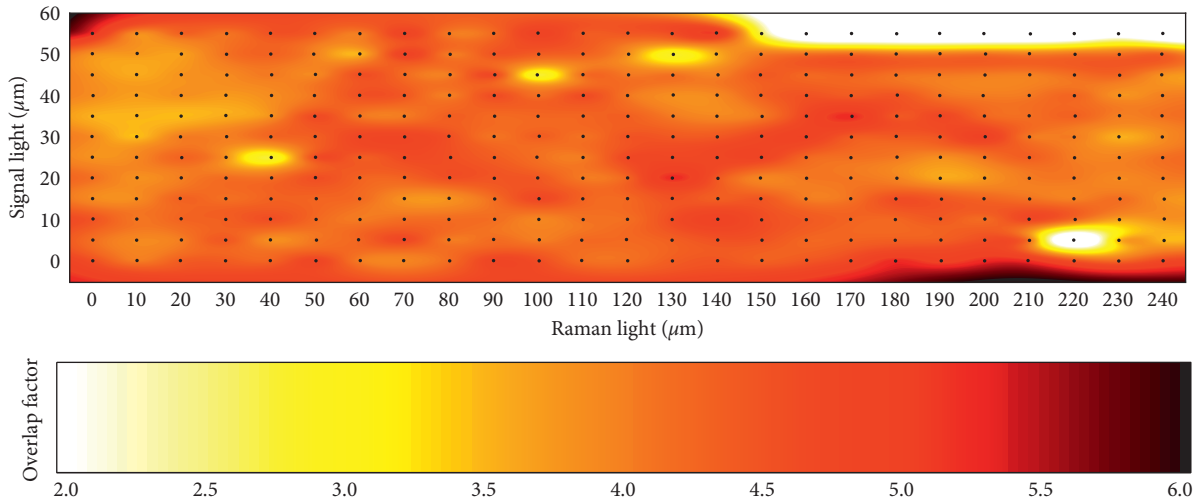

Figure 5: Mode distribution in the fibre with transverse distribution of the refractive index.

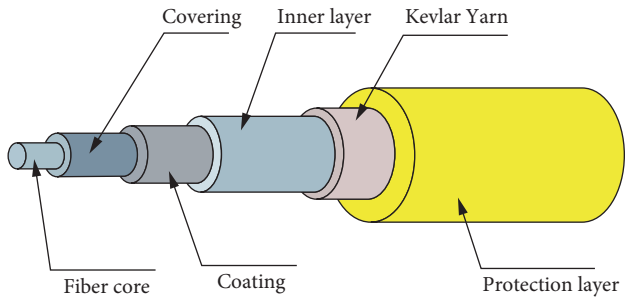

Figure 6: The fibre structure based on the geometric sensor signal enhancement technique.

that the various fibre designs are not opposed to each other means that a combination of design strategies is possible. By combining multiple strategies, such as introducing central partial doping into the spindle fibre design and improving large mode field fibre materials, SRS can be further suppressed and the output power of high-beam quality fibres can be increased.

3.2. SRS Transmission Characterisation Method. On the one hand, special optical fibre technology requires special fibre designs, which are relatively complex and expensive to prepare. On the other hand, fibres are an integral part of the laser system and the output laser performance is determined by all system components. Therefore, in addition to the use of special fibres, improving SRS transmission performance can also be achieved by optimising other system parameters (e.g., overall structure, pumping mode, and seed characteristics.) when building a high-power fibre laser system. As a common optical component, fibre gratings also demonstrate excellent Raman filtering properties.

3.2.1. Overall Structure. In order to suppress the SRS effect in kW-class multi-sensor signals, it is often necessary to use large mode field fibres (core diameter >20 μm) to reduce the fibre length and decrease the effective action distance. In 2017, Berto et al. [27] suggested that the effective action distance in dual-range amplification is twice as high as in single-range amplification, despite the fact that the fibre length is below 3 m. The intensity of SRS produced in a dual-range fibre amplifier with bidirectional pumping is comparable to that in a single-range amplifier with reverse pumping. In 2017, Wang et al. [28] investigated the SRS effect in a kilowatt cascade-pumped ytterbium-doped fibre amplifier. The model pointed out that although the Raman effect can be suppressed by lower doping concentrations and shorter fibre lengths, its effect on pump absorption and amplification efficiency should be considered. To avoid excessive pump light residuals, the fibre length should be greater than 50 m for pumping conditions with a central wavelength of 1018 nm.

3.2.2. Embedded with Multi-Sensor Enhancement Technology. The single oscillation cavity fibre laser system has the advantages of simple structural system and low production cost, and largely eliminates the damage to the laser system caused by material reflection. In order to increase the SRS threshold in a single oscillating cavity, the effect of the fibre Bragg grating (FBG), which is the core component of the oscillating cavity, on the SRS has been investigated. Lin showed that although the SRS can be suppressed by increasing the bandwidth of the OC-FBG, the increase in bandwidth will also increase the backward leakage power of the HR-FBG. In addition, the reflectivity of the OC-FBG in a single oscillating cavity structure also has an effect on the Raman light. The results show that the power of the Raman light decreases as the reflectivity of the OC-FBG decreases, but a low OC-FBG reflectivity leads to fluctuations in the output power due to the material reflecting back light into the resonant cavity. Analysis of transmission is based on filtered fibre optic gratings.

When Sun et al. [29] first used multiple long-period gratings (LPGs) in series to form a lumped filter, Raman fibre grating filters have gained widespread attention and developed rapidly due to their excellent Raman rejection ratio and relatively low insertion loss.

The principle of operation of a long-period grating is shown where Raman light of a specific wavelength is coupled and leaked to the cladding after the grating, and the corresponding transmission spectrum is shown in Figure 7. Earlier, Cheng et al. [30] wrote LPGs in a 10/125 μm fibre using a CO_2 laser and reduced the insertion loss of the 1030 nm signal light to 0.01 dB by a toe-cutting process, which made it possible to connect several gratings in series at the same time. In the experiment, the tandem of three long-period gratings doubled the SRS threshold and further additions to the number of gratings in tandem could be made to achieve better suppression. The resonance loss of the Raman light reached 26 dB, and the inscription of the long-period grating did not significantly affect the transmission loss of the signal light. The optimised 14/250 μm long-period grating was inserted into a MOPA laser system and achieved an SNR of 24 dB at 805 W output power.

In 2016, De et al. [31] first proposed the use of chirped tilted Bragg gratings to suppress SRS, as shown in Figure 8, where the chirped tilted Bragg grating suppresses Raman light by reflecting it backwards at an angle into the cladding compared to a long-period grating. Compared to long-period gratings, the spectrum of a chirped tilted Bragg grating is continuous and can be tuned by varying the tilt angle with relatively low sensitivity to the environment. However, the suppression principle of chirped tilted Bragg gratings allows (a) some of the reflected light to propagate backwards along the core, lowering the TMI threshold and causing non-linear effects such as four-wave mixing (FWM); (b) the light leaking from the tilted reflections to the cladding heats up the coating of the CTFBG, necessitating the addition of a cladding photo stripper (CPS) on the grating surface at high power, making the grating more difficult to fabricate, increasing the process difficulty, and reducing the lifetime of the grating. All-fibre single oscillators, kW-level LD-pumped fibre amplifiers, and kW-level cascaded fibre amplifiers have been implemented using chirped tilted Bragg gratings. The output spectra of the cascaded fibre amplifier with 0, 1, and 2 CTFBGs based on the multi-sensor signal are shown in Figure 8, and it can be seen that the SRS is significantly suppressed as the number of inserted chirped tilted Bragg gratings increases.

3.2.3. Analysis of Optical Fibre Transmission Based on Pumping Methods. The common pumping methods used in high-power multi-sensor signal systems are end-face pumping and distributed lateral pumping (DSCCP). In the end-face pumping method, the effective propagation distance of the high-power signal light is shorter (at the end of the Yb-doped fibre) in the backward pumping strategy, thus significantly reducing the distance between the signal light and Raman light and suppressing the SRS effect. Although the SRS threshold is lower for distributed lateral pumping compared to end-face pumping for the same fibre size, this pumping method results in a more uniform thermal load in the fibre and therefore significantly mitigates the thermal effects in the fibre. High-beam quality kW-class fibre oscillators and fibre amplifiers using distributed lateral pumping have also been implemented.

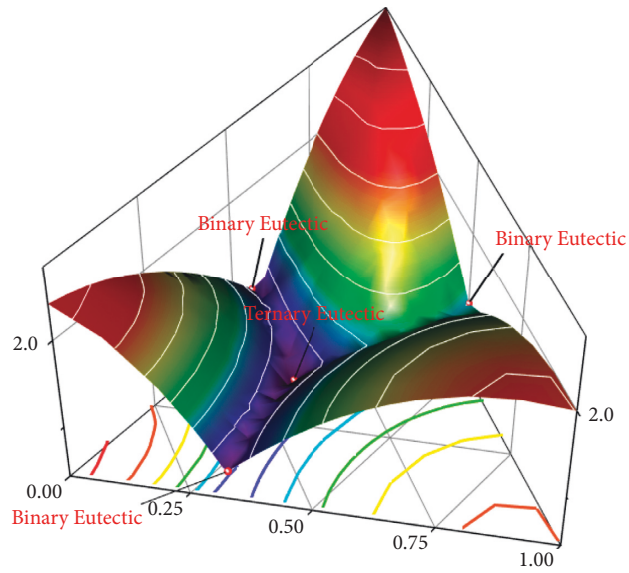

Figure 7: Raman light of a specific wavelength relationship of the corresponding transmission spectrum.

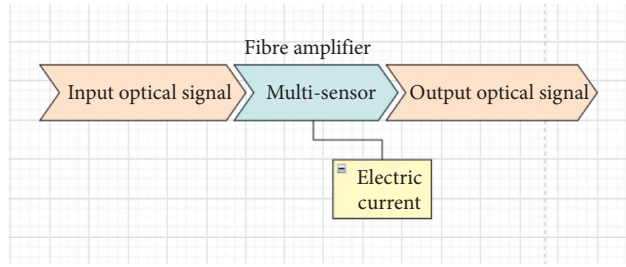

Figure 8: The cascaded fibre amplifier with CTFBGs based on the multi-sensor signal.

3.2.4. Transmission Analysis Based on Seed Characteristics and Self-Pulsation. In 2019, Koushki et al. [32] investigated the evolution of SRS with seed optical power in an Yb-doped fibre amplifier. The results showed that the SRS threshold was inversely proportional to the injected seed optical power. However, due to the limited pumping power, the reduction of the seed optical power decreases the output optical power. At the same time, the stability of the fibre optic amplifier is reduced by spontaneous radiation amplification (ASE) when it is operated at high power. In addition, studies have shown that ASE can also act as Raman seed light to cause Raman amplification, leading to a reduction in the SRS threshold. Lang et al. [33] investigated the effect of Raman scattering noise in the seed light on the SRS and gave a formula for calculating the Raman threshold of a high-power amplifier when considering Raman scattering noise in the seed light, showing that when the Raman scattering noise in the seed light is greater than 10–8 W, it plays an important role in the Raman threshold of the high-power amplifier.

Shi et al. [34] showed that in high-power continuous fibre lasers, relaxation oscillations can cause self-pulses with high peaks, which may trigger a series of non-linear effects such as SRS when their peak power reaches the non-linear threshold. According to Shi, the generation of self-pulses significantly

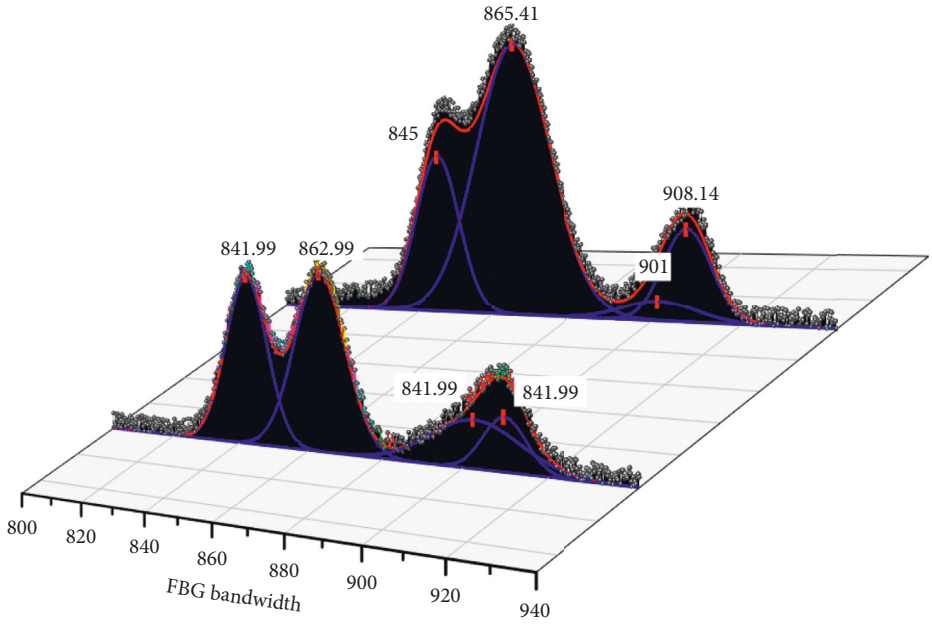

Figure 9: Corresponding simulation with combination of FBG bandwidth.

lowers the SRS threshold and mainly increases the forward Stokes optical power, so effective strategies are needed to suppress them. The commonly used improving SRS transmission performance includes using a single-frequency seed source with phase modulation, increasing the FBG bandwidth of the seed oscillation stage, and increasing the length of the energy transfer fibre between the seed and amplification stages. Figure 9 shows the corresponding simulation results, which show that the combination of FBG bandwidth increase and energy transfer fibre lengthening strategy can further suppress SRS. The combination of the two strategies results in a high SNR of ~50 dB at ~1 kW output power.

3.2.5. Analysis of Transmission Based on Four-Wave Mixing. In high-power multi-sensor signal systems, when the phase-matching conditions are met, photons at frequencies $\omega 1$ and $\omega 2$ pass through the parametric process to produce Stokes and anti-Stokes photons at frequencies $\omega 3$ and $\omega 4$. This process is called four-wave mixing (FWM) when the four frequencies are in the same fibre transverse mode in a few-mode fibre, or inter-mode four-wave mixing (IM-FWM) if they correspond to different fibre transverse modes. Shatarah et al. [35] showed that the normalised phase mismatch ΔB changes the effective Raman gain coefficient when FWM occurs

$$\begin{aligned} \Delta B &= \frac{(2\beta_L - \beta_S - \beta_a)}{g_0}, \\ \frac{g_{\text{eff}}}{g_0} &= \text{Re}\left[\sqrt{2(1 - f + f\chi_0) - \Delta B}\sqrt{\Delta B}\right], \\ g_{\text{eff}} &= \text{Re}\left[\sqrt{2(1 - f + f\chi_0) - \Delta B}\sqrt{\Delta B}\right] g_0, \\ X_0 &= 1.38i, \end{aligned} \tag{3}$$

where β_L, β_S, and β_a correspond to the propagation constants of the signal, Stokes, and Raman light; g_0 is the small-signal Raman gain coefficient; the value of the parameter f is 0.18; and $\chi_0 = 1.38i$ corresponds to the peak of the imaginary part of the Raman non-linear polarisation rate. The simulations suggest that the coupling between FMW and SRS may lead to a significant enhancement of SRS (~1.8 times), and therefore, a fibre with a suitable dispersion value needs to be selected to suppress SRS by optimising the parameter ΔB.

Gorelik et al. [36] theoretically analysed the effect of FWM and IM-FWM on RFL. Through the control variables method, the model states that FWM leads to a second-order Stokes optical power enhancement, which reduces the Raman threshold by 50%. Meanwhile, the effect of IM-FWM on RFL is explored by varying the power share of the LP11 mode in the seed light while ignoring FWM, and the results show that the Raman threshold decreases significantly as the power share of the LP11 mode increases, and IM-FWM has a stronger effect on the Raman threshold than FWM when the share is higher than 10^{-3}. The FWM can be effectively suppressed by adopting a time-domain stable pump source, while the IM-FWM can be suppressed by introducing higher-order mode losses.

The theoretical optimisation of the system parameters affecting the SRS threshold is summarised. It should be noted that, on the one hand, multi-sensor enhancement techniques cause changes in many important parameters that are often coupled with each other in affecting the SRS, and they in turn determine other characteristics of the laser system. Therefore, when designing the system, all factors should be taken into account in the context of the requirements and improving SRS transmission performance should not be pursued blindly.

4. Conclusion

As one of the main limiting factors for the single-link power increase of fibre laser systems, SRS increases the risk of system damage in addition to the reduction of system power and efficiency by backward Stokes light. In addition, a new phenomenon of mode degradation due to SRS has recently been observed in few-mode fibres. As a new physical characterisation of SRS in few-mode fibres, the available experimental results do not fully match the theoretical explanation and need further investigation. The study of strategies to enhance the transmission efficiency associated with combing SRS can, on the one hand, improve the power output of existing high-power, high-beam quality fibre laser systems; on the other hand, the dynamic adjustment of SRS intensity through multi-sensor means can help to deepen the understanding of the analytical methods for SRS transmission characteristics. As a result of continuous efforts by researchers, various Raman-enhanced transmission techniques have been developed and are now divided into two main categories: special fibre design techniques and overall system structure optimisation. The introduction of multi-sensor enhancement techniques in special fibre design techniques has shown excellent capabilities for improving transmission characteristics and high-power applications. In addition to the use of fibre gratings as Raman filtering components, the optimisation of the system structure is based on the influence of various sensor enhancement techniques (e.g., ASE, self-pulsing, and FWM) on the Raman light and the optimisation of the relevant parameters to achieve the upgrading of the transmission characteristics. In the next step, we will continue to explore the physical mechanism of SRS transmission characteristics optimisation and the corresponding analysis methods in conjunction with SRS transmission techniques based on multi-sensor enhancement techniques and mode decomposition techniques. The feasibility study of introducing new multi-sensor enhancement techniques will also be carried out to further enhance the power level of existing high-power, high-beam quality fibre laser systems to provide a reference.

Data Availability

The dataset can be accessed upon request.

Conflicts of Interest

The authors declare that they have no conflicts of interest.

References

[1] F. Yang, Y. Zhao, Y. Qi, and Y. Z. H. L. W. Tan, "Towards label-free distributed fiber hydrogen sensor with stimulated Raman spectroscopy," *Optics Express*, vol. 27, no. 9, pp. 12869–12882, 2019.

[2] M. Lawrence and J. A. Dionne, "Nanoscale nonreciprocity via photon-spin-polarized stimulated Raman scattering[J]," *Nature Communications*, vol. 10, no. 1, pp. 1–8, 2019.

[3] K. Jiao, J. Shu, H. Shen, and Z. F. R. Guan, "Fabrication of kW-level chirped and tilted fiber Bragg gratings and filtering of stimulated Raman scattering in high-power CW oscillators," *High Power Laser Science and Engineering*, vol. 7, p. e31, 2019.

[4] R. Ranjan, M. Indolfi, M. A. Ferrara, and L. Sirleto, "Implementation of a nonlinear microscope based on stimulated Raman scattering," *Journal of Visualized Experiments*, no. 149, Article ID e59614, 2019.

[5] M. Wang, Y. Zhang, Z. Wang, and J. J. J. X. X. Sun, "Fabrication of chirped and tilted fiber Bragg gratings and suppression of stimulated Raman scattering in fiber amplifiers," *Optics Express*, vol. 25, no. 2, pp. 1529–1534, 2017.

[6] K. Jiao, H. Shen, Z. Guan, and F. R. Yang, "Suppressing stimulated Raman scattering in kW-level continuous-wave MOPA fiber laser based on long-period fiber gratings," *Optics Express*, vol. 28, no. 5, pp. 6048–6063, 2020.

[7] M. Heck, V. Bock, R. G. Krämer et al., "Mitigation of stimulated Raman scattering in high powermulti-sensor signals using transmission gratings[C]//Fiber Lasers XV: technology and Systems," *International Society for Optics and Photonics*, vol. 10512, Article ID 105121I, 2018.

[8] D. Lioe, K. Mars, S. Kawahito, and K. K. T. M. Yasutomi, "A stimulated Raman scattering CMOS pixel using a high-speed charge modulator and lock-in amplifier," *Sensors*, vol. 16, no. 4, p. 532, 2016.

[9] K. Mars, D. X. Lioe, S. Kawahito, and K. K. T. M. Yasutomi, "Label-Free biomedical imaging using high-speed lock-in pixel sensor for stimulated Raman scattering," *Sensors*, vol. 17, no. 11, p. 2581, 2017.

[10] F. Yang and W. Jin, "All-fiber hydrogen sensor based on stimulated Raman gain spectroscopy with a 1550 nm hollow-core fiber[C]," in *Proceedings of the 2017 25th Optical Fiber Sensors Conference (OFS)*, pp. 1–4, IEEE, Jeju, South Korea, 24 April 2017.

[11] H. J. Lee, K.-C. Huang, G. Mei, and C. N. W. J. K. J. J.-X. Zong, "Electronic preresonance stimulated Raman scattering imaging of red-shifted proteorhodopsins: toward quantitation of the membrane potential," *The Journal of Physical Chemistry Letters*, vol. 10, no. 15, pp. 4374–4381, 2019.

[12] Y. Li, B. Shen, S. Li, Y. Zhao, J. Qu, and L. Liu, "Review of stimulated Raman scattering microscopy techniques and applications in the biosciences," *Advanced Biology*, vol. 5, no. 1, Article ID 2000184, 2021.

[13] Z. Amira, B. Mohamed, and E. Tahar, "Monitoring of temperature in distributed optical sensor: Raman and Brillouin spectrum," *Optik*, vol. 127, no. 8, pp. 4162–4166, 2016.

[14] M. Mehrabi, H. Beyranvand, and M. J. Emadi, "Multi-band elastic optical networks: inter-channel stimulated Raman scattering-aware routing, modulation level and spectrum assignment," *Journal of Lightwave Technology*, vol. 39, no. 11, pp. 3360–3370, 2021.

[15] Z. Wang, W. Yu, J. Tian, and T. D. Q. P. M. Qi, "5.1 kW tandem-pumped fiber amplifier seeded by random fiber laser with high suppression of stimulated Raman scattering," *IEEE Journal of Quantum Electronics*, vol. 57, no. 2, pp. 1–9, 2021.

[16] F. Yang, Y. Zhao, Y. Qi et al., "Label-free distributed hydrogen sensing with stimulated Raman scattering in hollow-core fibers[C]," in *Proceedings of the Optical Fiber Sensors*, Optical Society of America, Lausanne Switzerland, 24 September 2018.

[17] B. Manifold, E. Thomas, A. T. Francis, and A. H. D. Hill, "Denoising of stimulated Raman scattering microscopy images via deep learning," *Biomedical Optics Express*, vol. 10, no. 8, pp. 3860–3874, 2019.

[18] Y. Ozeki, T. Asai, J. Shou, and H. Yoshimi, "Multicolor stimulated Raman scattering microscopy with fast

wavelength-tunable Yb fiber laser," *IEEE Journal of Selected Topics in Quantum Electronics*, vol. 25, no. 1, pp. 1–11, 2019.

[19] V. S. Gorelik, P. P. Sverbil, V. V. Filatov, and D. G. T. S. H. Bi, "Transmission spectra of one-dimensional porous alumina photonic crystals," *Photonics and Nanostructures - Fundamentals and Applications*, vol. 32, pp. 6–10, 2018.

[20] F. Hu, L. Shi, and W. Min, "Biological imaging of chemical bonds by stimulated Raman scattering microscopy," *Nature Methods*, vol. 16, no. 9, pp. 830–842, 2019.

[21] S. Yan, S. Cui, K. Ke, and B. X. S. P. Zhao, "Hyperspectral stimulated Raman scattering microscopy unravels aberrant accumulation of saturated fat in human liver cancer," *Analytical Chemistry*, vol. 90, no. 11, pp. 6362–6366, 2018.

[22] X. Hu, W. Chen, M. Chen, and Z. Meng, "Experimental observation of the competition between stimulated Brillouin scattering, modulation instability and stimulated Raman scattering in long single mode fiber," *Journal of Optics*, vol. 18, no. 8, p. 085501, Article ID 085501, 2016.

[23] G. Sciortino, A. Ragni, A. De la Cadena, and M. G. D. G. Sampietro, "Four-channel differential lock-in amplifiers with autobalancing network for stimulated Raman spectroscopy," *IEEE Journal of Solid-State Circuits*, vol. 56, no. 6, pp. 1859–1870, 2021.

[24] Y. Yang, Y. Yang, Z. Liu, and L. S. X. Z. M. Guo, "Microcalcification-based tumor malignancy evaluation in fresh breast biopsies with hyperspectral stimulated Raman scattering," *Analytical Chemistry*, vol. 93, no. 15, pp. 6223–6231, 2021.

[25] W. Pei, H. Li, W. Huang, and M. Z. Wang, "All-fiber tunable pulsed 1.7 μm fiber lasers based on stimulated Raman scattering of hydrogen molecules in hollow-core fibers," *Molecules*, vol. 26, no. 15, p. 4561, 2021.

[26] D. S. Choi, B. J. Rao, D. Kim, and S.-H. H. M. Shim, "Selective suppression of CARS signal with three-beam competing stimulated Raman scattering processes," *Physical Chemistry Chemical Physics*, vol. 20, no. 25, pp. 17156–17170, 2018.

[27] P. Berto, C. Scotté, F. Galland, and H. H. B. Rigneault, "Programmable single-pixel-based broadband stimulated Raman scattering," *Optics letters*, vol. 42, no. 9, pp. 1696–1699, 2017.

[28] X. Wang, H. Qi, Y. Li, and F. H. F. Y. Z. X. X. Yu, "Synthesis and characterization of new Sr3(BO3)2 crystal for stimulated Raman scattering applications," *Crystals*, vol. 7, no. 5, p. 125, 2017.

[29] X. Sun, J. Li, and M. Hines, "SNR improvement in a Raman based distributed temperature sensing system using a stimulated Raman scattering filter[C]//Fiber Optic Sensors and Applications XIV," *SPIEL*, vol. 10208, pp. 69–74, 2017.

[30] T. Cheng, W. Gao, X. Xue et al., "Experimental observation of stimulated Raman scattering in a fluoride fiber[C]//Optical Components and Materials XIV," *SPIEL*, vol. 10100, pp. 363–368, 2017.

[31] L. De Xing, "A study on CMOS image sensors for stimulated Raman scattering using high-speed lateral electric field charge modulators[J]," *Dr. Diss*, 2016.

[32] E. Koushki and B. Maleki, "Induced photoacoustic gratings due to Raman scattering in organic components," *Dyes and Pigments*, vol. 164, pp. 82–86, 2019.

[33] X. Lang and K. Welsher, "Mapping solvation heterogeneity in live cells by hyperspectral stimulated Raman scattering microscopy," *The Journal of Chemical Physics*, vol. 152, no. 17, p. 174201, Article ID 174201, 2020.

[34] L. Shi, A. A. Fung, and A. Zhou, "Advances in stimulated Raman scattering imaging for tissues and animals," *Quantitative Imaging in Medicine and Surgery*, vol. 11, no. 3, pp. 1078–1101, 2020.

[35] I. S. M. Shatarah and R. Olbrycht, "Distributed temperature sensing in optical fibers based on Raman scattering: theory and applications[J]," *Measurement Automation Monitoring*, vol. 63, 2017.

[36] V. S. Gorelik, D. Bi, Y. P. Voinov, and A. I. V. A. A. I. Vodchits, "Spontaneous and stimulated Raman scattering in protium and deuterium water," *Optics and Spectroscopy*, vol. 126, no. 6, pp. 687–692, 2019.